E-Journal of Advanced Maintenance Vol.9-2 (2017) 60-65
Japan Society of Maintenology

R&D of Multi-Frequency ECT Algorithms for FBR SG Tubes

Ovidiu MIHALACHE, Toshihiko YAMAGUCHI, Takuma SHIRAHAMA and Masashi UEDA

Japan Atomic Energy, Sector of Fast Reactor Research and Development, Monju Project Management and Engineering Center,1 Shiraki, Tsuruga-shi, Fukui-ken, 919-1279, Japan

ABSTRACT

The adherence of sodium on the external surface of steam generator tubes of Fast Breeder Reactors adds an additional level of complexity in the in-service inspection of SGs using eddy current testing. The paper focusses on research and development of novel multi-frequency algorithms, based on eddy current signals, special developed and tuned to enhance the signal from defects located on external tube surface and to suppress electromagnetic noise from the conductive sodium and tube support plates. The application of the multi-frequency algorithm is investigated using both three-dimensional finite element simulations and experimental measurements from SG tubes soaked and then drained of sodium, in a sodium tank mock-up.

KEYWORDS

eddy currents, multi-frequency, steam generator, fast breeder reactor, three dimensional finite element, sodium

ARTICLE INFORMATION

Article history:
Received 7 November 2016
Accepted 27 April 2017

1. Introduction

One of the techniques used in FBR in the in-service inspection of steam generator tubes (SG) is the eddy current technique (ECT). One of the particularities of SG tubes in FBR is that they are soaked in sodium during reactor operation. In order to improve the defect detection technique, a multi-frequency ECT technique using the ECT signal at various frequencies is employed to enhance the signal/noise ratio. For ferromagnetic SG tubes it was shown that the remote field eddy current technique (RF-ECT) is sensitive to both inner and outer tube defects [1-2]. The application of multi-frequency ECT technique for SG tubes of nuclear power plant was also shown to be used for SG tubes of reactors [3-5], but without sodium and using eddy currents at higher frequencies, above 10 KHz frequency, and using less ECT at lower frequency (lower than 1 KHz) as in the RF-ECT.

Using the RF-ECT, new multi-frequency (MF) algorithms, devised for a bobbin coil configuration and named window-MF (WMF) and dynamic-window MF (DWMF), were previously presented and tested with either signals from two-dimensional or three-dimensional (3D) finite element (FE) simulations (both with/without sodium) or experimental data, but without sodium influence when used for helical SG tubes [6-9]. However, because defects are located on the SG tube outer surface the ECT signal changes due to the influence of the sodium accumulating inside defects.

In the present paper we extend the validation of these algorithms, WMF and DWMF, when using bobbin coils, with experimental RF-ECT measurements from defects located near the helical tube support plates in SG tubes similar with FBR tubes, in both cases when sodium covers or does not cover the tube surface. Further application of the method is also extended to the multi-coils detection units, but using three-dimensional FEM simulations, in order to improve the signal/noise ratio for detection of smaller outer tube partial defects.

2. Measurements and 3D FEM simulations of ECT signals for FBR SG tubes

A SG tank mock-up, with three SG tubes attached to large tube support plate (SP), is filled and then drained of sodium in order to obtain various sodium layers configurations around tube SP and outer tube defects (OD). WMF and DWMF algorithms are investigated and validated on these SG tubes, before and after sodium adheres to SG tube outer surface.

ISSN-1883-9894/10 © 2010 – JSM and the authors. All rights reserved.

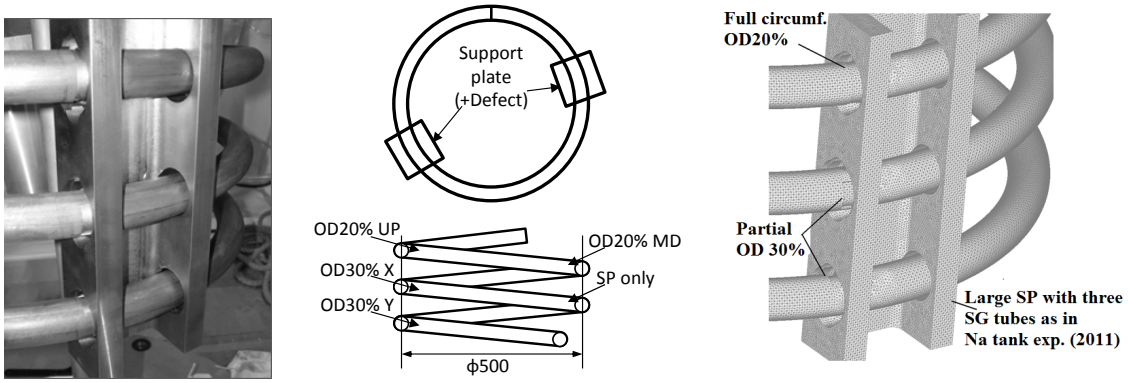

a) b) c)

Fig. 1. a) SG tubes with three defects (groove OD20%-upper tube, partial OD30%X-middle tube, partial OD30%-lower tube);b) SG schematics; c) 3D FEM simulation model

Fig. 2. RF-ECT system with various detection units: bobbin coil or multi-coils

In a previous paper [7-8], the authors investigated the formation of sodium layers and locations of sodium drops on the outer SG tube surface, after sodium draining, in a controlled sodium tank mock-up. Three SG tubes similar (geometry and material characteristics: made of Cr-Mo alloy with a 3.8 mm wall thickness) to FBR tubes, as seen in Fig. 1, are inserted through a larger tube SP. The above configuration rests in a 2 meter diameter larger sodium mockup-tank that surrounds the helical tubes, tank that is filled with sodium at high temperature (500^0C) and then is drained successively, in order to obtain various sodium configurations. After each sodium drain and cooling down to room temperature, the ECT signal from detection coils is recorded for various outer tube defects, grooves OD20%tw (tube wall thickness) and partial OD30%tw on different location of tubes, that are located near and under tube SP. The detection unit of the RF-ECT system is presented in Fig. 2 and consists in either bobbin coil or multi-system coils.

3. Principles of multi-frequencies algorithms

Multi-frequency (MF) algorithm emphasizes the defect signal and reduces the background noise by synthesizing the ECT signals at two or more different frequencies. In the standard linear procedure the combination of two ECT signals is performed by following equation:

$$S = S_1 + \alpha \cdot R(\varphi) \cdot S_2 \quad (1)$$

where S_1 and S_2 are measurement data (real and imaginary components) at two frequencies, while α is the amplitude coefficient of the signal and R(φ) is the rotation matrix for the Lissajous image in Fig. 3(left), that rotates the signal with phase φ. Fig. 3(left) shows an example of application of MF algorithm, where SP measured signal is considered as a noise while the defect signal in the ”SP+Defect” configuration is the signal that is enhanced by MF algorithm.

In opposition to the MF algorithm that is applied to the all set of data in the Lissajous-form, the window multi-frequency algorithm sets a window-band and is applied to a reduced window-data [7-9]. Fig. 3(right) shows the principle of WMF. The upper part of the figure shows the arrangement of the SG tube and location of defect under the tube helical support plate. The middle part shows the defect detection data as it is measured, and how for each subsequently window data, the MF is applied. The lower part shows the results of the WMF algorithm where the position of S/N ratio localize the

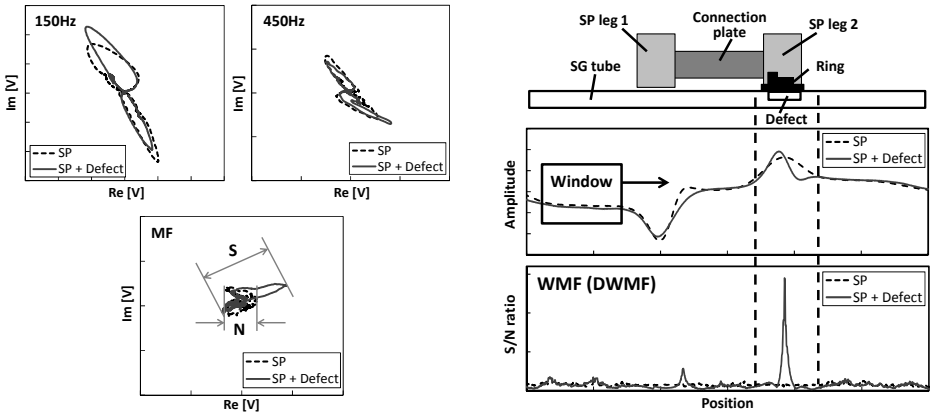

Fig. 3. Standard MF algorithm in Lissajous representation using 2 ECT frequencies (left image). Principle of WMF or DWMF algorithms (right image)

defect area with a larger S/N ratio. The parameters of the WMF algorithms are previously determined and then fixed during scanning window. Therefore, in order to determine the optimum WMF parameters, it is required to check the results of calculations for various windows size and set one that is optimum for the particular ECT sensor used to acquire the data. Meanwhile, the dynamic-window multi-frequency (DWMF) changes its parameters dynamically at each point of the window scan, and searches the parameters S/N when this ratio is maximized. Consequently, by using DWMF it is possible to simplify the determination operations of the optimum multi-frequency parameters in normal WMF. These are accomplished by finding the most optimum parameters along the scan and use their mean value as a starting point for the WMF algorithm.

The dynamical "window" algorithm (see Eq. 2), described also in [8], uses a fixed-size and smaller subset data of length "w" from signal of length "n" at two frequencies $S_1(1,n)$ and $S_2(1,n)$. These signals are combined using a standard MF algorithm for each window "w" resulting in the signal S_i. The DWMF signal S_w (i) at each "i" point of the signal is defined by the maximum ratio S_i/N_i where N_i is the signal of noise.

$$S_i = S_1(i,i+w) + \alpha \cdot R(\varphi) \cdot S_2(i,i+w), \quad N_i = N_1(i,i+w) + \alpha \cdot R(\varphi) \cdot N_2(i,i+w),$$
$$S_w(i) = Max(S_i / N_i) \ \ when \ \ \alpha = 1/10..10, \ \ \varphi = 0..2\pi, \ \ i = 1, n-w \qquad (2)$$

4. Validation of WMF with measurements using bobbin-coil system

Because of the sodium high electrical conductivity, after each sodium drain different sodium layers or sodium filling the defects will add an additional noise ECT signal. In the WMF algorithm noise is considered the signal from both sodium and tubes SP. The WMF algorithm maximizes the defect signal against this noise, and in the present paper it is investigated that when using experimental measurements an optimized solution can be found and validated with a signal/noise ratio larger than 2.

Fig. 4 and 5 show the result of applying the WMF and DWMF to directly experimental measurements (150Hz-450Hz) for OD20% groove and OD30% partial described earlier, defects that are always hidden under SP as in Fig. 1 (right). Each of these figures shows the results of "No sodium" (that was the configuration of SG tubes before sodium was drained) and also the "1st drain", (that were configurations of tubes after sodium was drained 1st time). For example, in the "No sodium" results in Fig. 4, the upper image represents the real ECT measurement data (real component at 150 Hz), the middle picture shows the WMF analysis, while the lower picture represents the DWMF results, respectively. The WMF results in Fig. 4,5 were obtained by using the most optimal MF parameters in equation 2, using a brute force attack where the phase ranged between 0 to 360 degrees with 2 degree step while the amplification factor ranged between 1/10 to 10 with a 0.2 step.

When focusing on the influence of the sodium drain on the MF algorithms, it can be seen that both WMF and DWMF are relatively stable, without large reduction in S/N ratio, this being illustrated

with results after each three sodium drains. It was found out that the largest S/N ratio peaks in the area where the defect is present. Other S/N peak`s ratio larger than 2 were in a zone that corresponds to the start position of the support plate. This is because a defect influence actually extends up to 80 mm to the start of SP, but despite this 2nd peak signal, it is considered that there is no significant impact on the detection defect.

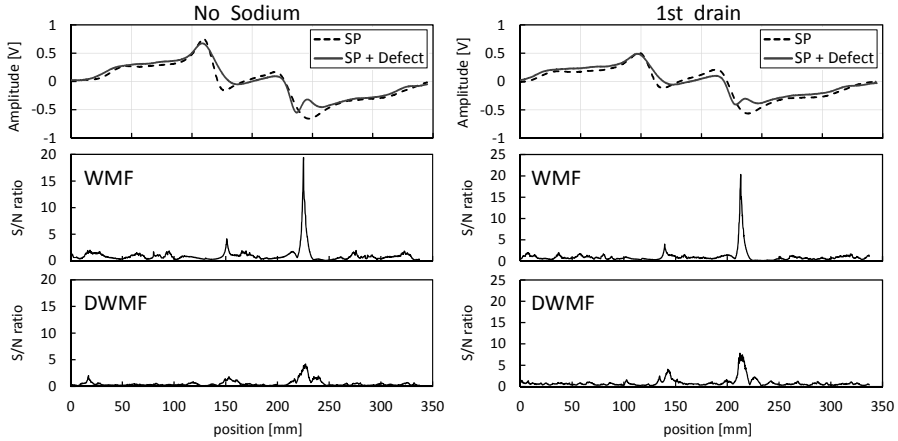

Fig. 4. Result of applying the WMF and DWMF for full circumferential groove OD20%

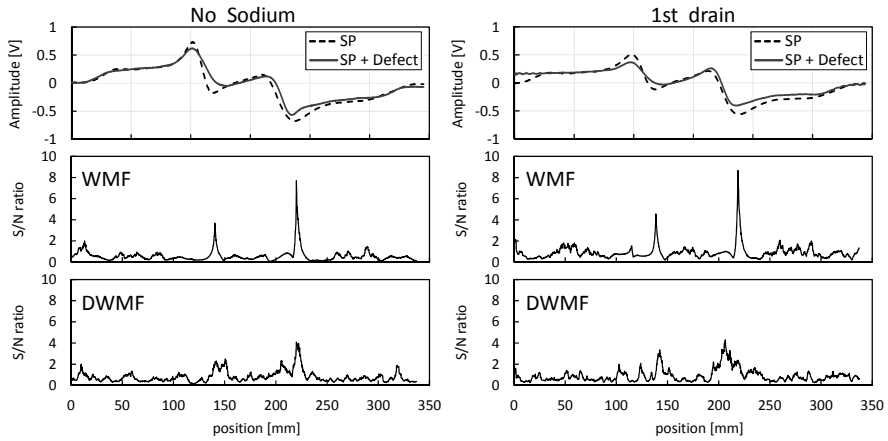

Fig. 5. Result of applying the WMF and DWMF for partial OD30%

Table 1 Peak S/N ratio of WMF and DWMF for partial OD30%

Sodium drain	Peak S/N ratio					
	WMF with multifrequency parameters					DWMF
	φ = 178 α = 3.2 (No-sodium)	φ = 202 α = 2.8 (1st-drain)	φ = 184 α = 3.4 (2nd-drain)	φ = 192 α = 3.2 (3rd-drain)	φ = 193 α = 3.1 (Average)	
No-Sodium	**7.70**	3.45	5.73	4.42	**4.49**	**4.09**
1st-drain	3.71	**8.66**	4.46	7.81	**7.39**	**4.30**
2nd-drain	5.56	6.06	**7.02**	5.85	**5.70**	**5.42**
3rd-drain	6.39	5.83	6.64	**7.69**	**7.10**	**4.36**

Table 1 shows S/N peak values of WMF with optimum-find multi-frequency parameters and DWMF with dynamical parameters. The WMF results are shown with five sets of parameters. The first four sets correspond to the "no sodium" and after three sodium drains, while the last one is the medium average of all of them. In addition, when applying WMF, with other than the most-optimum parameter (for example using data from "1st drain" but with parameters of WMF determined at "no sodium" case) the S/N peak is reduced to about 1/5th of maximum value in the worst case, but still high above 2. DWMF algorithms are faster in finding the optimal parameters than WMF, therefore being more advantageous and easy to detect the defect location.

5. WMF using 3D FEM simulated data for multi-coil system

DWMF algorithms (window-size equal with 7 mm) were applied to three-dimensional FEM simulations described previously [7-8] to the multi-coils unit of the RF-ECT device. Fig. 6 shows the C-scan of the outer tube surface near tube support at 60 Hz in the absence or presence of sodium.

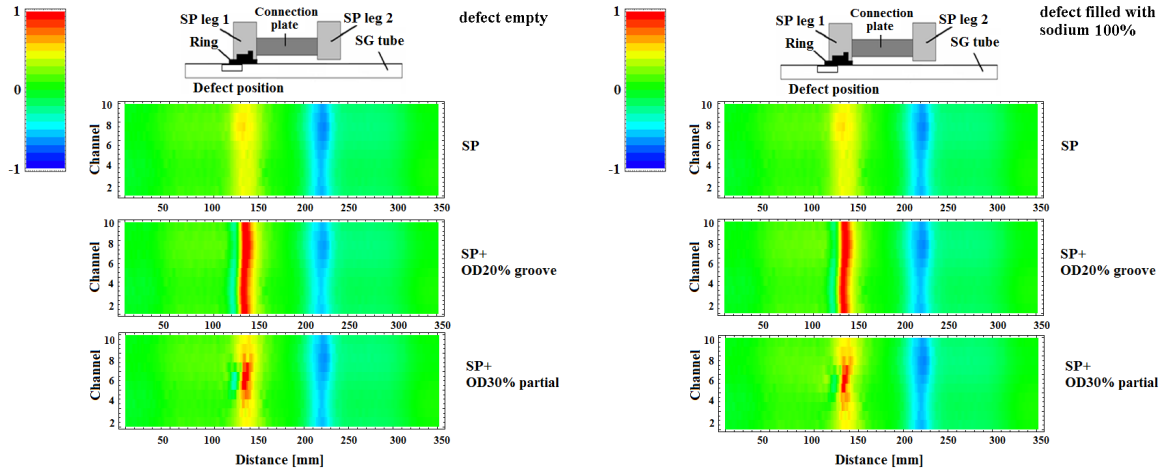

Fig. 6. FEM simulations of C-scan of ECT signal at 60Hz using multi-coil unit when defect is empty of sodium (left image) or filled 100% with sodium (right image)

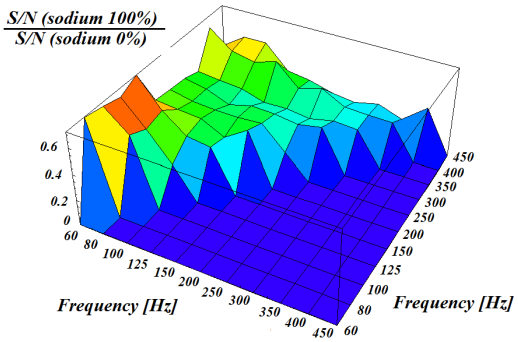

Fig. 7. S/N ratio for various WMF algorithms using multi-coil unit and 100% sodium filling of OD30%

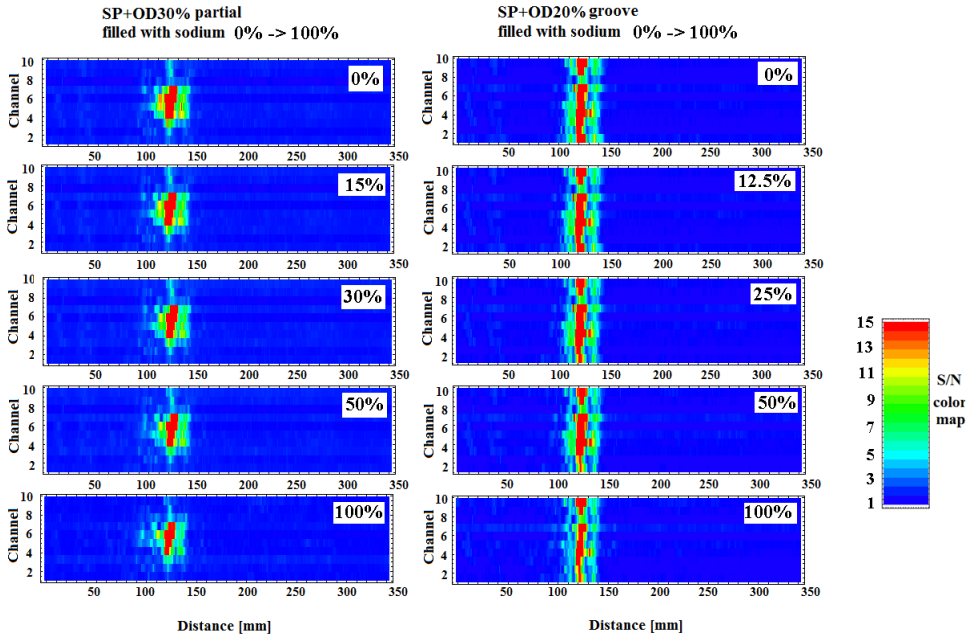

Fig. 8. Application of WMF algorithm (60Hz-150Hz) for multi-coil unit using 3D FEM simulations

While at a single ECT frequency, both defect and support signal are visible on the C-scan image, in the MF algorithm it is required to suppress any signal but defect signal, independently of sodium accumulation percentage inside the defect. 3D FEM numerical simulations were conducted at various frequencies (60Hz to 450 Hz) to find the optimum DWMF algorithm that is the least sensitive to the presence of sodium. Results, presented in Fig. 7, show that an algorithm can be found using the frequency set 60Hz-150Hz, in which the signal/noise ratio changes maximum 30% (0.7 value) when sodium fills 100% the defect. Application of the DWMF for the optimized frequency set (see Fig. 8) therefore validates the sensitivity of defect detection, even for partial outer defect OD30%tw, with a large signal/noise ratio up to 15, when defects are filled 100% with sodium.

6. Conclusions

Windows multi-frequency and dynamic-windows MF algorithms were applied directly to experimental ECT signals from bobbin coils for FBR SG tubes that were drained of sodium, with outer defects localized near tube support plates. The results confirmed that it can be found multi-frequency algorithms at (150Hz-450Hz) that provide a high signal/noise ratio up to 8 (for WMF) or 5 (for DWMF). These algorithms do not depend by the sodium accumulated near SP or inside defects volumes. The S/N peak position indicates the location of the defect. While WMF shows slightly better S/N ratio, DWMF is a more convenient and faster algorithm that was proved to be equal stable and insensitive to sodium noise signal.

By using three dimensional FEM simulations it was shown that DWMF algorithm can also be applied to multi-coils detection units. When choosing the optimized set of frequencies (60Hz-150Hz) in the MF algorithm, large S/N ratio (S/N >15) could be found for detection of both groove OD20%tw and partial OD30%tw when located under tube SP, even in the presence of sodium that is filling the defect, confirming DWMF stability.

References

[1] D. L. Atherton, S. Sullivan and M. Daly, A remote field eddy current tool for inspecting nuclear reactor pressure tubes, Br. J. Nondestructive Testing, 30, pp. 22-28, (1988).

[2] H. Fukutomi, T. Takagi and M. Nishikawa, Remote field eddy current technique applied to non-magnetic steam generator tubes, NDT&E International, 34,pp. 17-23, (2001).

[3] S. Kumano, N. Kawase, K. Kawata and A. Kurokawa, Signal processing of rotating pancake eddy current signal for steam generator tubes, Proceedings of the 13th International Conference on NDE in the Nuclear and Pressure Vessel Industries, Kyoto, Japan, 22-25 May, pp. 413-420, (1995).

[4] V. Ganugapati, K. Arunchalam, P. Ramuhalli, L.Udpa and S.Udpa, A polynomial mixing algorithm for suppressing TSP signals in bobbin coil eddy current data, Electromagnetic Nondestructive Evaluation (VII), Studies in Applied Electromagnetics and Mechanics 26, (2006), pp. 213-219.

[5] Zhenmao Chen, Naoki Chigusa, Hiromu Isaka and Kenzo Miya, Data processing of corrosion noise polluted ECT signals for heat exchanger tubes of Cu-Ni alloy, Electromagnetic Nondestructive Evaluation (VIII), Studies in Applied Electromagnetics and Mechanics, 24, (2004), pp 128-135.

[6] O. Mihalache, T. Yamaguchi, M. Ueda , "Computational Challenges in Numerical Simulations of ISI of Ferritic Steam Generator Tubes in Fast Breeder Reactors using Eddy Currents and Multi-frequency Algorithms", E-Journal of Advanced Maintenance, Vol. 3, No. 2, pp. 54-77, August, (2011).

[7] O. Mihalache, T. Yamaguchi, M. Ueda, "Validations of Multifrequency ECT Algorithms for Helical SG Tubes of FBR", Electromagnetic Nondestructive Evaluation (XVII), Vol. 39, pp. 109-119, (2014).

[8] O. Mihalache, T. Yamaguchi, M. Ueda, "Multifrequency ECT for Sodium Drained SG Tubes of FBR using 3D Finite Element Simulations", 17thISEM , Kobe, Sept , (2015).

[9] T. Yamaguchi, O. Mihalache, M. Ueda, "Experimental Measurements and Simulations of ECT Signal for Ferromagnetic SG Tubes Covered by a Sodium Layer", Electromagnetic Nondestructive Evaluation, (XVII), Vol 39, pp. 144-154, (2014).